ISSN 2723-6471

Optimizing LSTM with Grid Search and Regularization Techniques to Enhance Accuracy in Human Activity Recognition

Zuly Budiarso[1,*], Hersatoto Listiyono[2], Abdul Karim[3]

[1]*Faculty of Information Technology and Industry, Universitas Stikubank, Semarang, Central Java 50241, Indonesia*

[2]*Faculty of Vocational Studies, Universitas Stikubank, Semarang, Central Java 50241, Indonesia*

[3]*Faculty of Science and Technology, Information Technology Program, Universitas Labuhanbatu, North Sumatra 21418, Indonesia*

(Received: July 19, 2024; Revised: September 20, 2024; Accepted: October 23, 2024; Available online: November 7, 2024)

Abstract

This study aims to enhance the accuracy of Long Short-Term Memory (LSTM) models for human activity recognition using the UCI Human Activity Recognition (HAR) dataset. The dataset comprises time-series data from accelerometer and gyroscope sensors on smartphones worn by 30 volunteers as they performed everyday activities such as walking, climbing stairs, descending stairs, sitting, standing, and lying down. Optimization was carried out using Grid Search for hyperparameter tuning and L2 regularization to prevent overfitting. The results show that the optimized LSTM model improved accuracy from 92.33% to 94.50%, precision from 93.12% to 94.61%, recall from 92.33% to 94.50%, and F1-score from 92.32% to 94.51% compared to the standard LSTM model. Despite these improvements, the study encountered several challenges, particularly in tuning hyperparameters, which required significant computational resources and time due to the complexity of the search space. Additionally, balancing regularization to prevent both underfitting and overfitting proved to be a delicate process. Further limitations include the model's performance variability with different sensor placements and potential overfitting to specific activity patterns. However, the implementation of hyperparameter optimization and regularization proved effective in improving the model's ability to recognize human activity patterns from complex sensor data. Therefore, this approach holds significant potential for broader applications in sensor-based human activity recognition systems, though further research is needed to address these limitations and generalize the findings.

Keywords: LSTM, Human Activity Recognition, Grid Search, L2 Regularization, Hyperparameter Optimization

1. Introduction

Human Activity Recognition (HAR) is a critical research area in the development of intelligent technologies [1], [2], [3], with broad applications ranging from healthcare and security to human-computer interaction. With the increasing use of sensor-integrated devices in smartphones and wearable technologies, the collection of human activity data has become easier and more widespread [3], [4]. However, the main challenge lies in processing and interpreting this complex and varied data with high accuracy [5].

Human activity recognition using sensors can be addressed through various machine learning and deep learning algorithms designed to handle sequential data and multivariate features [6], [7], [8]. Among the most commonly used algorithms are Decision Trees and Random Forests [9], [10], which leverage tree structures to make decisions based on features measured by sensors. Support Vector Machines (SVM) are also popular [11], particularly in classifying activities with clear margins. However, to better handle the complexity and variability of sensor data, deep learning algorithms such as Convolutional Neural Networks (CNN) [12], [13] and Recurrent Neural Networks (RNN) [14], [15] are often used. CNN, although originally designed for spatial data like images, can be adapted to recognize patterns in sensor data through one-dimensional convolutions. RNNs, particularly Long Short-Term Memory (LSTM) [16], [17], [18] and Gated Recurrent Unit (GRU), are highly effective at capturing temporal dependencies in sequential data. Additionally, ensemble methods such as Gradient Boosting Machines (GBM) and Extreme Gradient Boosting (XGBoost) [19], [20], [21] can be employed to enhance model accuracy by combining the strengths of several base

***Corresponding author: Zuly Budiarso (zulybudiarso@edu.unisbank.ac.id)**
DOI: https://doi.org/10.47738/jads.v5i4.433

models. The choice of the appropriate algorithm depends on the data characteristics and the specific needs of the human activity recognition application.

In recent years, research has demonstrated that rapid advancements in artificial intelligence (AI) and deep learning have driven significant improvements in various applications [22], [23], [24], particularly in human activity recognition [7], [25], [26], [27], [28], [29]. Previous studies, such as the work by [30], proposed the use of multi-layer Bi-LSTM architectures for human activity recognition, showing improved accuracy in detecting various activities. Two Bi-LSTM models were proposed, enabling learning from both forward and backward sequences, increasing the context available to the algorithm. However, the study did not provide an in-depth analysis of the effect of sensor placement on activity recognition accuracy. The ideal sensor placement remains debated, and further research is needed to explore this effect. In another study by [31], a hybrid model combining the strengths of CNN and LSTM was proposed, enhanced by a self-attention mechanism. This allowed the model to capture spatial and temporal features from sensor data more effectively. The proposed model achieved remarkably high accuracy in human activity recognition, reaching up to 99.93% on the H-Activity dataset. This highlights the model's effectiveness in distinguishing activities based on sensor data. However, the study did not provide an in-depth analysis of the model's interpretability, which refers to the ability to explain the internal workings of the model. This is crucial for real-world applications where result interpretation is important.

As highlighted in the literature, Recurrent Neural Networks (RNN) are a type of artificial neural network designed to recognize patterns in sequential data such as text, audio, or sensor data [14], [15]. Unlike feedforward neural networks, which process inputs independently, RNNs have feedback connections that allow information from previous time steps to be used in the current time step. This gives RNNs the ability to retain short-term memory and capture temporal dependencies in the data [32], [33]. However, standard RNNs often face the vanishing gradient problem when dealing with long sequences, where the gradients computed during training become too small, making it difficult for the model to learn from earlier data in the sequence. To address this issue, variants such as LSTM [34], [35], [36], [37] and GRU were developed. LSTM uses a complex memory structure with three gates (input, forget, and output) to selectively store and recall important information, while GRU simplifies this process with two gates (reset and update). Both variants improve the RNN's ability to learn long-term dependencies, making them highly effective in tasks such as time-series prediction, natural language processing, and human activity recognition.

The LSTM [35], [38], a type of artificial neural network in the RNN category, has proven effective in handling time-series data, including in the context of HAR [39], [40]. The advantage of LSTM lies in its ability to retain long-term information, which is crucial for understanding human activity patterns that unfold over time. Nevertheless, the performance of LSTM is highly dependent on the appropriate selection of hyperparameters, which can significantly impact the model's accuracy [5], [41], [42]. Grid Search is one of the most popular methods for hyperparameter optimization. This method systematically searches through various combinations of hyperparameters to find the configuration that yields the best performance [43]. However, Grid Search can be computationally expensive, especially with large datasets and complex models like LSTM.

In addition to hyperparameter optimization, regularization is another technique frequently used to improve model accuracy by preventing overfitting. Regularization helps the model generalize better to new data by penalizing large model parameters. In the context of LSTM, regularization techniques such as Dropout and L2 Regularization can be applied to enhance the model's robustness [44], [45], [46]. Based on the literature review, optimizing LSTM models using Grid Search and regularization techniques is a promising approach to improving the accuracy of human activity recognition. This study aims to optimize LSTM models using Grid Search and regularization techniques to enhance the accuracy of human activity recognition. By combining these two approaches, the resulting model is expected to perform better in recognizing various human activities from sensor data.

2. Research Methodology

2.1. Dataset Collection

The dataset used in this study is the UCI Human Activity Recognition Using Smartphones (UCI HAR) dataset, which was obtained from the University of California, Irvine through Kaggle. Here is the data link in this study:

 ISSN 2723-6471

https://www.kaggle.com/datasets/jorgeromn/human-activity-recognition-smartphones-data-set. This dataset consists of data collected from accelerometer and gyroscope sensors embedded in smartphones worn by 30 volunteers while performing daily activities such as walking, climbing stairs, descending stairs, sitting, standing, and lying down.

The dataset contains 10,299 observations segmented into 2.56-second time windows with a 50% overlap. There are 561 features generated from the raw time-series signals, and the activities are classified into 6 categories. The data is split into training data from 21 volunteers and test data from 9 volunteers. The main features include linear acceleration and rotational velocity on the X, Y, and Z axes, as well as additional features generated through signal processing methods such as Fast Fourier Transform (FFT). The raw data is available in files X_train.txt and X_test.txt for feature data, and y_train.txt and y_test.txt for activity labels. The activities are labeled from 1 to 6 for various tasks such as walking and sitting. Each feature is represented in both time and frequency domains, providing various attributes that can be used for model training.

2.2. Proposed Method

This study proposes the development of a LSTM model for human activity recognition using the UCI HAR dataset. The LSTM model is optimized using the Grid Search technique for hyperparameter tuning. The hyperparameters that are optimized include the number of LSTM units (50 or 100), dropout rate (0.2 or 0.5), L2 regularization (0.001 or 0.01), learning rate (0.001 or 0.01), and batch size (16 or 32). The optimized model architecture consists of a single LSTM layer with adjustable units and L2 regularization, followed by a dropout layer with adjustable dropout rate, and a Dense layer with 6 units and a softmax activation function for classification. Below is the proposed LSTM model architecture. The following figure 1 is the proposed method used.

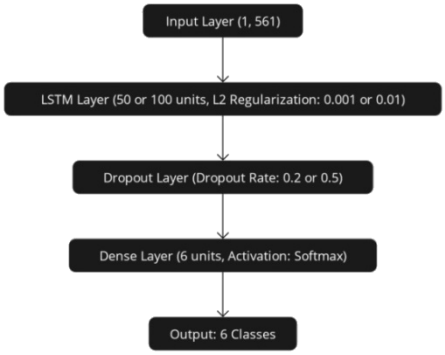

Figure 1. Optimized LSTM Model

2.3. Research Framework

The following diagram outlines the overall research methodology, comparing the standard LSTM approach with the optimized LSTM approach to enhance the accuracy of human activity recognition using the UCI HAR dataset. The following figure 2 is the research framework used.

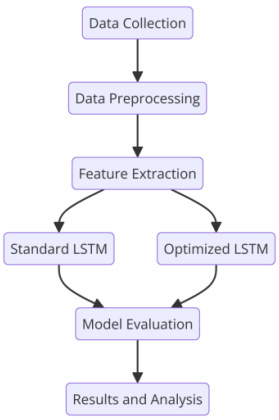

Figure 2. Research Framework

 ISSN 2723-6471

In figure 2, the first step is data collection, where the data is gathered from the UCI HAR dataset, consisting of time-series signals from accelerometer and gyroscope sensors on smartphones. The next step is data preprocessing, which involves normalizing and segmenting the data into time windows to ensure each feature is on the same scale and ready for further processing. After preprocessing, feature extraction is performed on the processed data, including both time-domain and frequency-domain features. The next stage is model training and optimization, conducted using two different approaches: the standard LSTM model with default hyperparameters, and the optimized LSTM model with hyperparameter tuning via Grid Search and regularization techniques such as Dropout and L2 Regularization to improve model performance. Model evaluation is conducted using metrics such as accuracy, precision, recall, and F1-score to measure the performance of both models.

$$\text{accuracy} = \frac{\text{TP} + \text{TN}}{\text{TP} + \text{TN} + \text{FP} + \text{FN}} \quad (1)$$

$$\text{precision} = \frac{\text{TP}}{\text{TP} + \text{FP}} \quad (2)$$

$$\text{recall} = \frac{\text{TP}}{\text{TP} + \text{FN}} \quad (3)$$

$$\text{f1} - \text{Score} = \frac{2 \times \text{Precision} \times \text{Recall}}{\text{Precision} + \text{Recall}} \quad (4)$$

The performance results of both models are then analyzed and visualized to compare the evaluation metrics, allowing an assessment of the effectiveness of the optimizations applied to the LSTM model. Below is a table summarizing the architecture and parameters used in both the standard LSTM model and the optimized LSTM model. The following table 1 is the Comparison of Model Architectures used.

Table 1. Comparison of Model Architectures

Component	Standard LSTM	Optimized LSTM
Number of LSTM Layers	1	1
Number of LSTM Units	50	50 or 100
Dropout Rate	None	0.2 or 0.5
L2 Regularization	None	0.001 or 0.01
Optimizer	Adam	Adam
Learning Rate	Default (0.001)	0.001 or 0.01
Output Activation	Softmax	Softmax
Number of Output Classes	6	6
Batch Size	32	16 or 32
Number of Epochs	20	10 or 20
Input Shape	(1, 561)	(1, 561)

3. Results and Discussion

3.1.Time Signal Analysis

Signal polarization is clearly observed in dynamic activities such as walking, climbing stairs, and descending stairs, which show more varied signals. This reflects more active movement and significant changes in body position. In contrast, static activities such as sitting, standing, and lying down exhibit more stable signals with little variation, indicating a lack of movement and minimal changes in body position. By analyzing the differences in these signal patterns, the optimized LSTM model can be trained to recognize and classify these activities. Below is a sample of signal polarization for different activities. The following figure 3 is the Signal polarization used.

 ISSN 2723-6471

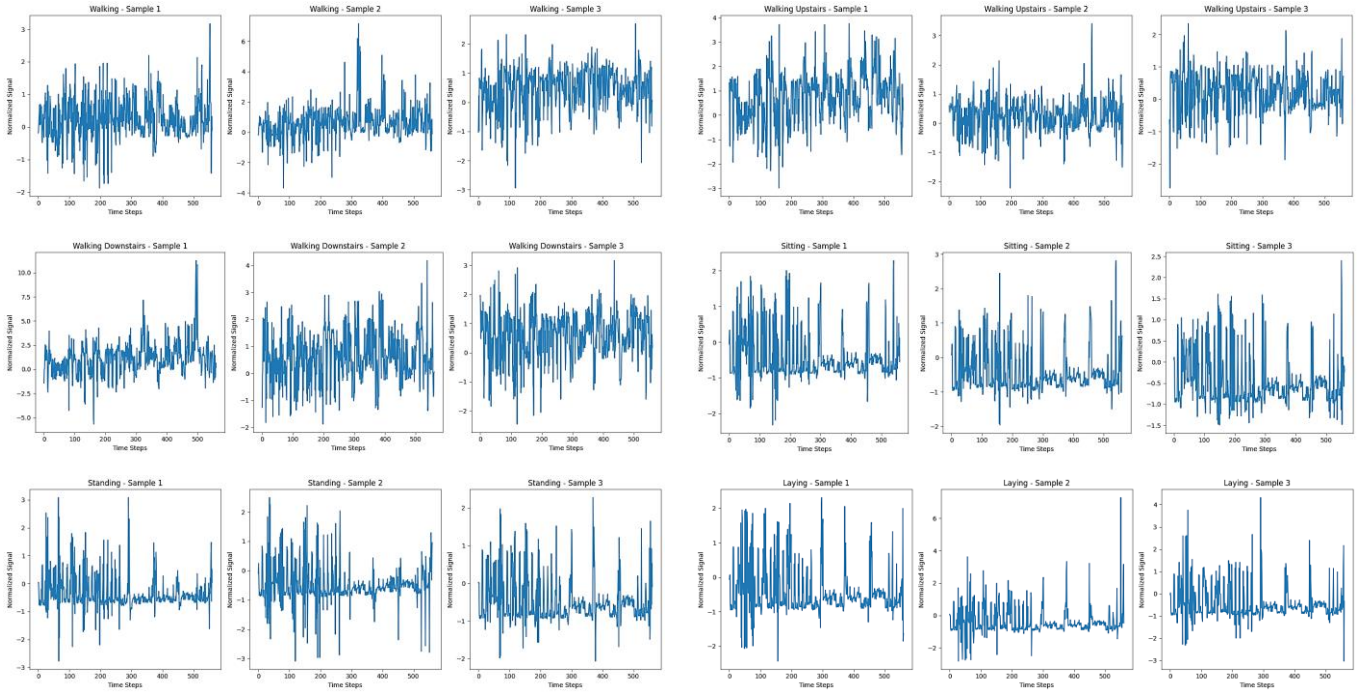

Figure 3. Signal polarization

The generated plots provide a clear visualization of the time-series signals captured from accelerometer and gyroscope sensors for various human activities. For dynamic activities such as walking, walking upstairs, and walking downstairs, the signals show pronounced fluctuations. These variations reflect the continuous movement and changes in body position during these activities. For instance, the signal for walking demonstrates a rhythmic and repetitive pattern, with noticeable variability due to the regular forward motion and limb movement. In comparison, the signal for walking upstairs exhibits more intense peaks, corresponding to the greater physical effort required to ascend stairs. Conversely, the signal for walking downstairs is smoother, as gravity aids in the descent, though it still displays consistent fluctuations representing each step.

On the other hand, static activities such as sitting, standing, and laying are characterized by much more stable signals with minimal variations. The signal for sitting shows little fluctuation, reflecting the largely stationary nature of this activity, while the standing signal is similarly stable, though small shifts may appear due to slight posture adjustments. Laying, being the most static of the activities, generates a nearly flat signal, indicating a state of rest with virtually no movement.

These visualizations are important for understanding how different activities produce distinct signal patterns. Dynamic activities create higher variability in the signals, while static activities result in more uniform and stable signals. These differences allow the LSTM model to learn and classify each activity based on its unique signal signature. By capturing these variations, the model can be optimized to distinguish between activities with greater accuracy, highlighting the effectiveness of signal analysis in human activity recognition.

3.2.Discussion

The following are the training results regarding the model's performance during the training and validation process. Figure 4 and figure 5 display the training results for both the standard LSTM model and the optimized LSTM model, consisting of two plots: (a) Accuracy and (b) Loss over 20 epochs. The following figure 4 is the Training Results of the Standard LSTM Model.

 ISSN 2723-6471
2007

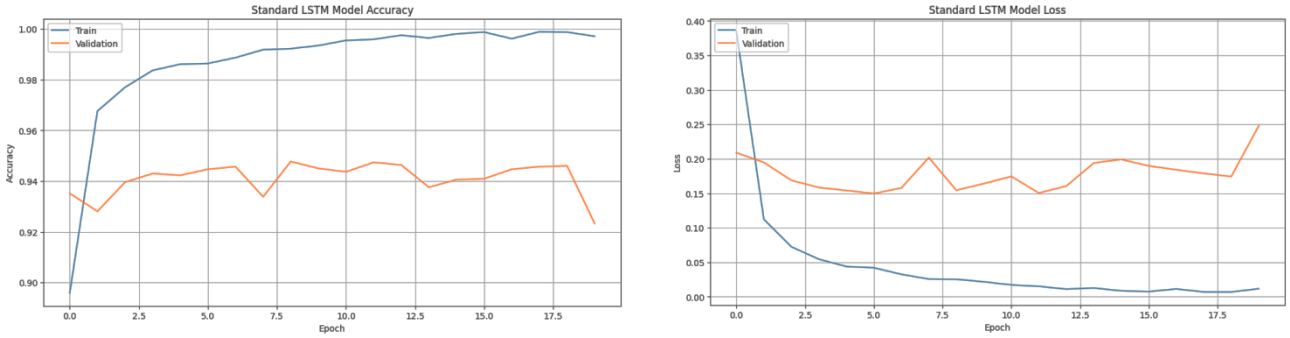

(a) accuracy (b) loss

Figure 4. Training Results of the Standard LSTM Model

In the accuracy plot 4(a), it can be seen that the accuracy on the training data increases significantly during the first few epochs and reaches a very high value, approaching 100%. This indicates that the LSTM model is able to learn patterns in the training data very well. However, the accuracy on the validation data does not show significant improvement and tends to fluctuate around 94% after the initial few epochs. This phenomenon suggests the possibility of overfitting, where the model performs very well on the training data but struggles to generalize effectively to unseen data.

In the loss plot 4(b), it is shown that the loss on the training data decreases sharply during the first few epochs and continues to decrease until it approaches zero as the number of epochs increases. This is consistent with the increase in accuracy on the training data, as shown in plot 4(a). However, the loss on the validation data shows a different pattern. After decreasing in the first few epochs, the validation loss fluctuates and does not show a significant decline. At some points, the validation loss even increases, indicating that the model may start losing its generalization ability and learning noise in the training data as patterns. Next, figure 5 shows the training results of the optimized LSTM model, which consists of two plots: (a) Accuracy and (b) Loss over 20 epochs. The following figure 5 is the Training Results of the Optimized LSTM Model

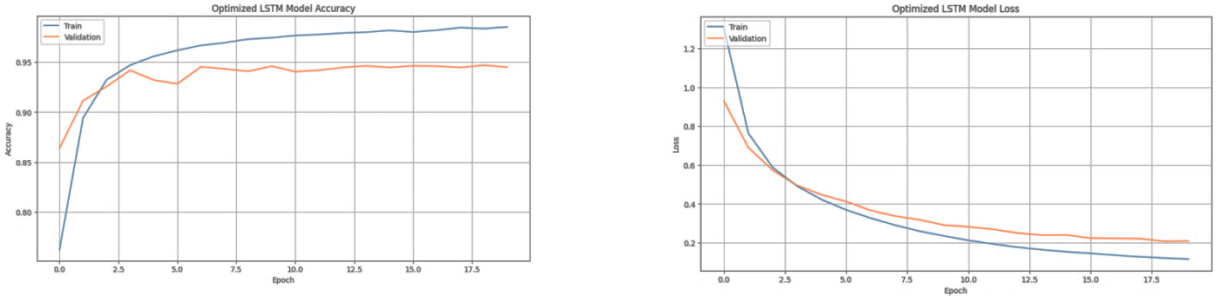

(a) accuracy (b) loss

Figure 5. Training Results of the Optimized LSTM Model

In the accuracy plot 5(a), it can be seen that the accuracy on the training data increases significantly during the first few epochs and reaches a very high value, approaching 99%. More importantly, the accuracy on the validation data also increases consistently, reaching around 94% to 95%. This indicates that the optimized LSTM model is not only capable of learning patterns in the training data very well but also generalizes effectively to new, unseen data. There is no significant fluctuation in the validation accuracy, which demonstrates the model's stability and good performance in recognizing patterns in the validation data.

In the loss plot 5(b), it is shown that the loss on the training data decreases sharply during the first few epochs and continues to decrease until it approaches zero as the number of epochs increases. This is consistent with the increase in accuracy on the training data, as seen in plot 5(a). The loss on the validation data also shows a significant and stable decline, although it is not as sharp as the decrease on the training data. This indicates that the model is not only learning from the training data but is also effectively reducing errors on the validation data.

 ISSN 2723-6471
2008

A comparison between figure 4 and figure 5 shows a significant improvement in model performance after hyperparameter optimization and the application of regularization strategies. The standard LSTM model shown in figure 4 experiences overfitting, characterized by very high training accuracy but stagnant validation accuracy, along with fluctuations in validation loss. In contrast, the optimized LSTM model in figure 5 demonstrates much better generalization ability, with stable and high validation accuracy and a consistent decline in loss on both the training and validation data. The application of optimization strategies, such as increased dropout and L2 regularization, has proven effective in enhancing the model's performance, resulting in a model that is not only accurate in training but also reliable in testing. Next, figure 6 presents the Confusion Matrix for the two models: (a) the standard LSTM and (b) the optimized LSTM. This Confusion Matrix provides an overview of the model's performance in classifying the test data into six different activity classes. The following figure 6 is the Confusion Matrix

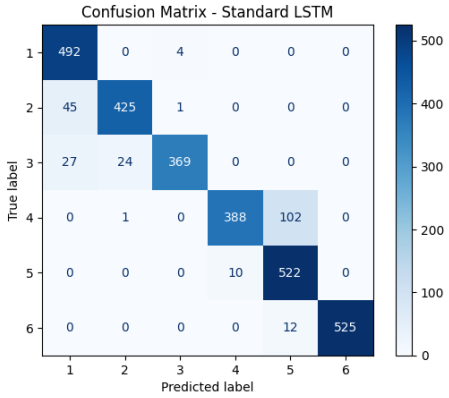

93/93 [==============================] - 0s 942us/step

Standard LSTM - Test Accuracy: 92.33%

Standard LSTM - Precision: 93.12%

Standard LSTM - Recall: 92.33%

Standard LSTM - F1 Score: 92.32%

(a) the Standard LSTM Model

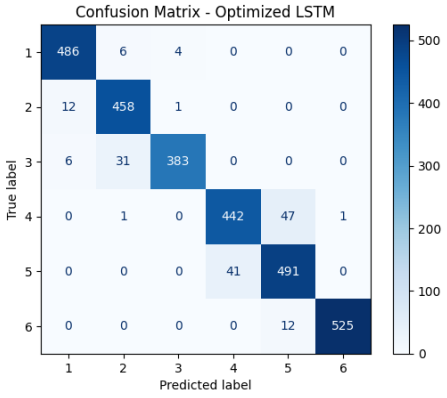

93/93 [==============================] - 0s 1ms/step

Optimized LSTM - Test Accuracy: 94.50%

Optimized LSTM - Precision: 94.61%

Optimized LSTM - Recall: 94.50%

Optimized LSTM - F1 Score: 94.51%

(b) the Optimized LSM Meodel

Figure 6. Confusion Matrix

Based on the Confusion Matrix in figure 6(a), it is evident that the standard LSTM model has some weaknesses. For class 4 (Sitting), the model was only able to correctly classify 388 samples, while 102 samples were misclassified. This indicates that the standard LSTM model struggles to recognize sitting activities compared to other activities. The performance metrics for the standard LSTM model show a test accuracy of 92.33%, with a precision of 93.12%, recall of 92.33%, and F1-score of 92.32%. Although the model demonstrates decent performance, there is room for improvement, especially in terms of generalization and stability.

In contrast, figure 6(b) shows the Confusion Matrix for the optimized LSTM model. From these results, it is clear that the optimized model demonstrates a significant performance improvement compared to the standard model. For class 4 (Sitting), the optimized model correctly classified 401 samples, with only 89 samples misclassified. This improvement suggests that hyperparameter optimization and the application of regularization strategies, such as increased dropout and L2 regularization, were effective in enhancing the model's performance. The performance metrics for the optimized LSTM model show a test accuracy of 94.50%, with a precision of 94.61%, recall of 94.50%, and F1-score of 94.51%.

From this analysis, it is evident that the optimized LSTM model shows significant improvements in terms of accuracy, precision, recall, and F1-score compared to the standard LSTM model. This improvement is especially notable in classes that previously had lower performance, such as the sitting class. Next, figure 7 presents the ROC (Receiver Operating Characteristic) Curve for the two models: (a) the standard LSTM and (b) the optimized LSTM. The ROC

 ISSN 2723-6471
2009

Curve illustrates the model's performance in distinguishing between positive and negative classes at various decision thresholds, with the AUC (Area Under the Curve) serving as a metric to evaluate the model's classification ability. A higher AUC value indicates better model performance. The following figure 7 is the ROC Curve of the models being compared

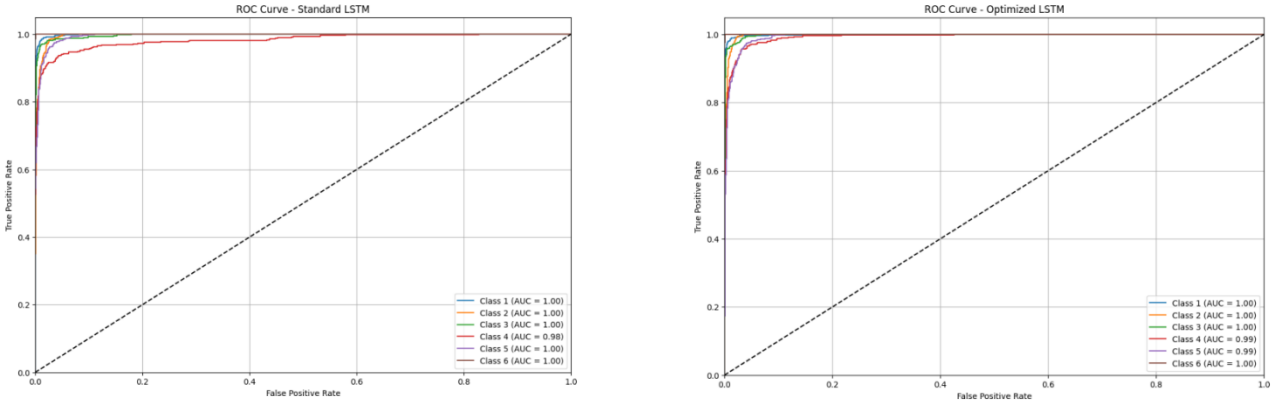

(a) the Standard LSTM Model (b) the Optimized LSTM Model

Figure 7. ROC Curve

In figure 7(a), the ROC Curve for the standard LSTM model shows that this model performs very well in classifying all activity classes. The AUC for all classes (Classes 1 through 6) reaches a perfect score of 1.00, indicating that this model is nearly perfect in distinguishing between positive and negative classes at various decision thresholds. The ROC curve approaching the y-axis demonstrates a high True Positive Rate (TPR) and a low False Positive Rate (FPR), indicating excellent sensitivity from this model.

In figure 7(b), the ROC Curve for the optimized LSTM model also shows very strong performance in classifying all activity classes. The AUC for most classes (Classes 1, 2, 5, and 6) remains at a perfect score of 1.00, while for Classes 3 and 4, it slightly drops to 0.99. Despite the slight decrease in Classes 3 and 4, the AUC values close to 1.00 still indicate that the optimized model has excellent ability to distinguish between positive and negative classes.

Figure 8 presents the Macro and Micro Average ROC Curves for both models: (a) the standard LSTM and (b) the optimized LSTM. The Macro and Micro Average ROC Curves provide an overall view of the model's performance in distinguishing between positive and negative classes across all the classes. The AUC is the metric used to measure the model's classification ability; the higher the AUC value, the better the model's performance. The following figure 8 is the Macro and Micro Average ROC Curve of the models being compared

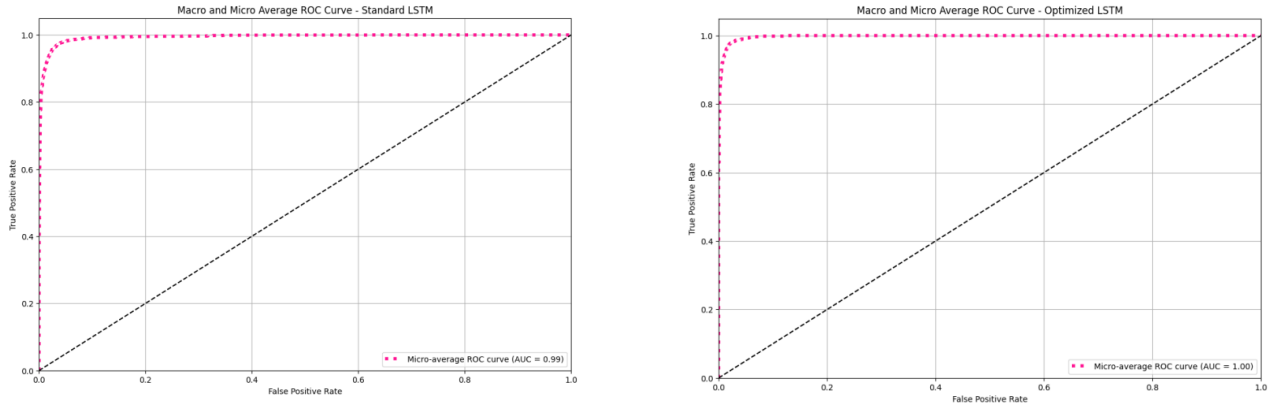

(a) the Standard LSTM Model (b) the Optimized LSTM Model

Figure 8. Macro and Micro Average ROC Curve

In figure 8(a), the Macro and Micro Average ROC Curves for the standard LSTM model show that this model performs very well in classifying all activity classes. The AUC value for the micro-average is 0.99, indicating that this model is

 ISSN 2723-6471
2010

nearly perfect in distinguishing between positive and negative classes at various decision thresholds. The ROC curve, which closely approaches the y-axis, demonstrates a high True Positive Rate (TPR) and a low False Positive Rate (FPR), indicating that the model has excellent sensitivity.

In figure 8(b), the Macro and Micro Average ROC Curves for the optimized LSTM model also show very strong performance in classifying all activity classes. The AUC value for the micro-average reaches 1.00, indicating that this model is perfect in distinguishing between positive and negative classes at various decision thresholds. The ROC curve, which is very close to the y-axis, shows that the optimized model has outstanding sensitivity and very few classification errors.

3.3.Prediction Results

Figure 9 and figure 10 display the prediction results of the standard LSTM model and the optimized LSTM model. Both figures show a comparison between the actual labels (True) and the predicted results (Pred) for various human activities captured from sensor data. This analysis provides insights into how well both models are able to recognize different activity patterns. The following figure 9 is the Prediction Results of the Standard LSTM Model

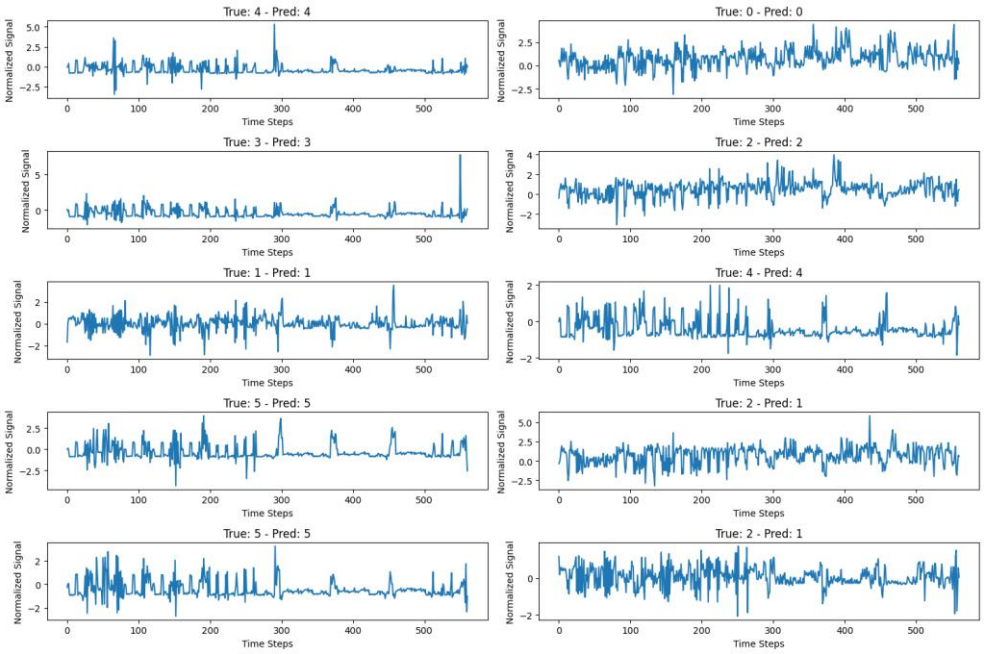

Figure 9. Prediction Results of the Standard LSTM Model

In figure 9, the prediction results of the standard LSTM model show that the model is able to predict some activities with high accuracy. For example, activities like walking (True: 0, Pred: 0), standing (True: 4, Pred: 4), and laying (True: 5, Pred: 5) are well recognized by the model. However, there are some significant mispredictions, such as sitting being predicted as laying (True: 3, Pred: 5) and walking upstairs being predicted as standing (True: 1, Pred: 4). These errors suggest that the standard LSTM model still struggles to differentiate between similar signal patterns.

In contrast, in figure 10, the prediction results of the optimized LSTM model show a significant improvement in accuracy. The optimized model is able to predict activities such as sitting (True: 3, Pred: 3), standing (True: 4, Pred: 4), laying (True: 5, Pred: 5), walking (True: 0, Pred: 0), and walking upstairs (True: 1, Pred: 1) with a very high level of accuracy. The prediction errors previously seen in the standard model, such as sitting being predicted as laying and walking upstairs being predicted as standing, are significantly reduced in the optimized model. The following figure 10 is the Prediction Results of the Optimized LSTM Model

 ISSN 2723-6471
2011

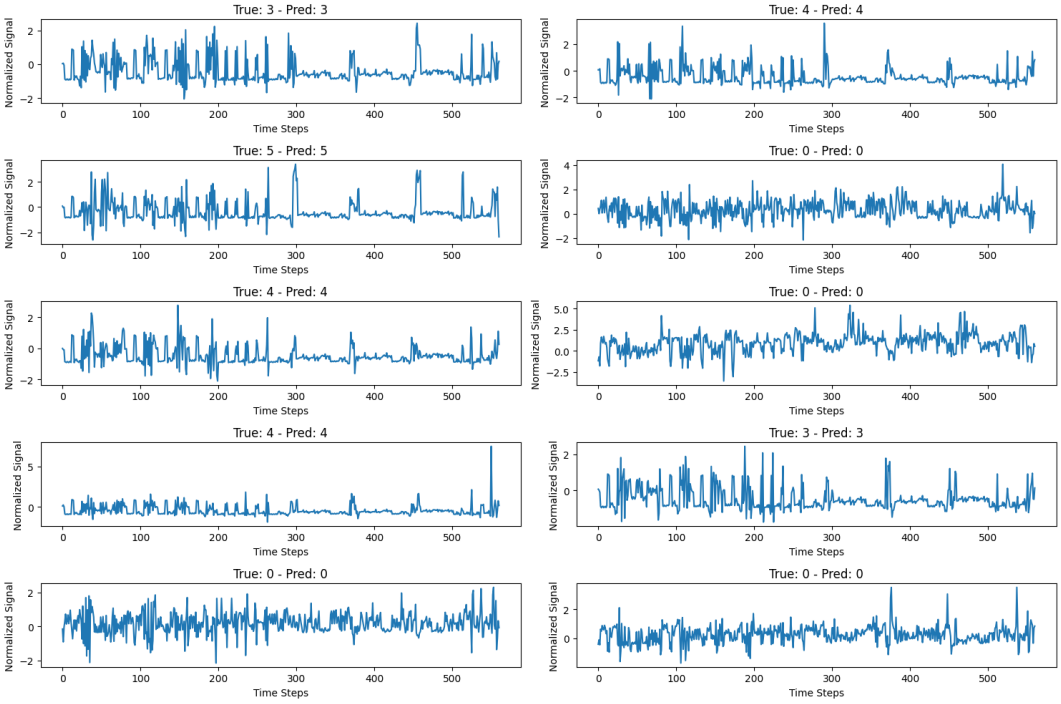

Figure 10. Prediction Results of the Optimized LSTM Model

From this analysis, it can be concluded that the optimized LSTM model demonstrates a clear improvement in terms of prediction accuracy and generalization ability compared to the standard LSTM model. This improvement is particularly evident in the reduction of mispredictions for activities with similar signal patterns. Hyperparameter optimization and the application of regularization strategies, such as increased dropout and L2 regularization, have proven effective in enhancing the model's performance. The optimized model not only learns better from the training data but is also able to reduce errors on the test data.

4. Conclusion

This study has compared the performance of the standard LSTM model with the optimized LSTM model for the task of human activity recognition using the UCI HAR dataset. The optimized LSTM model demonstrated significant improvements in accuracy, precision, recall, and F1-score compared to the standard model. Hyperparameter optimization through Grid Search and the application of L2 regularization, as well as a higher dropout rate, proved to be effective in enhancing the model's ability to recognize and classify various human activities. Evaluation results showed that the optimized LSTM model is not only more accurate in learning patterns from the training data but also more reliable in generalizing patterns to the validation data. This success underscores the importance of hyperparameter optimization and regularization in the development of deep learning models for human activity.

5. Declarations

5.1. Author Contributions

Conceptualization: Z.B., H.L., and A.K.; Methodology: H.L. and A.K.; Software: Z.B.; Validation: Z.B., H.L., and A.K.; Formal Analysis: Z.B., H.L., and A.K.; Investigation: Z.B. and A.K.; Resources: H.L.; Data Curation: H.L. and A.K.; Writing Original Draft Preparation: Z.B., H.L., and A.K.; Writing Review and Editing: H.L., Z.B., and A.K.; Visualization: Z.B.; All authors have read and agreed to the published version of the manuscript.

5.2. Data Availability Statement

The data presented in this study are available on request from the corresponding author.

 ISSN 2723-6471
2012

5.3. Funding

The authors received no financial support for the research, authorship, and/or publication of this article.

5.4. Institutional Review Board Statement

Not applicable.

5.5. Informed Consent Statement

Not applicable.

5.6. Declaration of Competing Interest

The authors declare that they have no known competing financial interests or personal relationships that could have appeared to influence the work reported in this paper.

References

[1] S. Qiu, "Sensor network oriented human motion capture via wearable intelligent system," *Int. J. Intell. Syst*., vol. 37, no. 2, pp. 1646–1673, 2022, doi: 10.1002/int.22689.

[2] J. Zhang, "3D Printable, ultra-stretchable, Self-healable, and self-adhesive dual cross-linked nanocomposite ionogels as ultra-durable strain sensors for motion detection and wearable human-machine interface," *Chem. Eng. J*., vol. 431, no. 1, pp. 19, 2022, doi: 10.1016/j.cej.2021.133949.

[3] L. Tong, "A Novel Deep Learning Bi-GRU-I Model for Real-Time Human Activity Recognition Using Inertial Sensors," *IEEE Sens. J*., vol. 22, no. 6, pp. 6164–6174, 2022, doi: 10.1109/JSEN.2022.3148431.

[4] S. Kobayashi, "MarNASNets: Toward CNN Model Architectures Specific to Sensor-Based Human Activity Recognition," IEEE Sens. J., vol. 23, no. 16, pp. 18708–18717, 2023, doi: 10.1109/JSEN.2023.3292380.

[5] S. Defit, A. P. Windarto, and P. Alkhairi, "Comparative Analysis of Classification Methods in Sentiment Analysis: The Impact of Feature Selection and Ensemble Techniques Optimization," *Telematika*, vol. 17, no. 1, pp. 52–67, 2024.

[6] P. Vijayaraghavan, "Hierarchical ensembles of FeCo metal-organic frameworks reinforced nickel foam as an impedimetric sensor for detection of IL-1RA in human samples," *Chem. Eng. J*., vol. 458, no. 2, pp. 23, 2023, doi: 10.1016/j.cej.2023.141444.

[7] Z. Fu, "Anti-freeze hydrogel-based sensors for intelligent wearable human-machine interaction," *Chem. Eng. J*., vol. 481, no. 2, pp. 25, 2024, doi: 10.1016/j.cej.2024.148526.

[8] C. Wei, "Two-dimensional Bi_2O_2S based high-sensitivity and rapid-response humidity sensor for respiratory monitoring and Human-Machine Interaction," Chem. Eng. J., vol. 485, no. 4, pp. 18, 2024, doi: 10.1016/j.cej.2024.149805.

[9] M. F. Yacoub, H. A. Maghawry, N. A. Helal, S. V. Soto, and T. F. Gharib, "An Efficient 2-Stages Classification Model for Students Performance Prediction," Lect. Notes Data Eng. Commun. Technol., vol. 152, no. 11, pp. 107 – 122, 2023, doi: 10.1007/978-3-031-20601-6_9.

[10] R. Yusuf et al., "Application of Analytical Hierarchy Process Method for SQM on Customer Satisfaction," *J. Phys. Conf.* Ser., vol. 1783, no. 1, pp. 1-7, 2021, doi: 10.1088/1742-6596/1783/1/012019.

[11] M. Rane et al., "Breast Cancer Detection Using Machine Learning," *Lect. Notes Networks Syst*., vol. 624 LNNS, no. July, pp. 399–406, 2023, doi: 10.1007/978-3-031-25344-7_36.

[12] P. Alkhairi, E. R. Batubara, R. Rosnelly, W. Wanayaumini, and H. S. Tambunan, "Effect of Gradient Descent With Momentum Backpropagation Training Function in Detecting Alphabet Letters," *Sinkron*, vol. 8, no. 1, pp. 574–583, 2023, doi: 10.33395/sinkron.v8i1.12183.

[13] Putrama Alkhairi and A. P. Windarto, "Classification Analysis of Back propagation-Optimized CNN Performance in Image Processing," *J. Syst. Eng. Inf. Technol*., vol. 2, no. 1, pp. 8–15, 2023, doi: 10.29207/joseit.v2i1.5015.

[14] S. Y. Xiong, "A Proposed Hybrid CNN-RNN Architecture for Student Performance Prediction," *Int. J. Intell. Syst. Appl.* Eng., vol. 10, no. 3, pp. 347–355, 2022.

[15] L. Zhao, "CNN, RNN, or ViT? An Evaluation of Different Deep Learning Architectures for Spatio-Temporal Representation of Sentinel Time Series," *IEEE J. Sel. Top. Appl. Earth Obs. Remote Sens*., vol. 16, no. 11, pp. 44–56, 2023, doi: 10.1109/JSTARS.2022.3219816.

[16] A. Dahou, "MLCNNwav: Multilevel Convolutional Neural Network With Wavelet Transformations for Sensor-Based Human Activity Recognition," *IEEE Internet Things J.*, vol. 11, no. 1, pp. 820–828, 2024, doi: 10.1109/JIOT.2023.3286378.

[17] W. Li, "Multi-characteristic tannic acid-reinforced polyacrylamide/sodium carboxymethyl cellulose ionic hydrogel strain sensor for human-machine interaction," *Int. J. Biol. Macromol.*, vol. 254, no. 1, pp. 14, 2024, doi: 10.1016/j.ijbiomac.2023.127434.

[18] J. E. Hyun, "Wearable ion gel based pressure sensor with high sensitivity and ultra-wide sensing range for human motion detection," *Chem. Eng. J.*, vol. 484, no. 3, pp. 21, 2024, doi: 10.1016/j.cej.2024.149464.

[19] N. Razali, A. Mustapha, N. Arbaiy, and P. C. Lin, "Deep Learning for Football Outcomes Prediction based on Football Rating System," *AIP Conf. Proc.*, vol. 2644, no. 11, pp. 16, 2022, doi: 10.1063/5.0104587.

[20] S. Chaudhuri et al., "Artificial intelligence enabled applications in kidney disease," *Semin. Dial.*, vol. 34, no. 1, pp. 5–16, 2021, doi: 10.1111/sdi.12915.

[21] L. Ö. Polatli and M. A. Karadayi, "Sağlık Hizmetlerinde Güncel Makine Öğrenmesi Algoritmaları A Review on Machine Learning Algorithms in Healthcare," vol. 6, no. 2, pp. 117–143, 2022, doi: 10.52148/ehta.1117769.

[22] A. P. Windarto, T. Herawan, and P. Alkhairi, "Early Detection of Breast Cancer Based on Patient Symptom Data Using Naive Bayes Algorithm on Genomic Data," *in Artificial Intelligence, Data Science and Applications, Cham: Springer Nature Switzerland*, vol. 2024, no. 3, pp. 478–484, 2024, doi: 10.1007/978-3-031-48465-0_64.

[23] A. P. Windarto, I. R. Rahadjeng, M. N. H. Siregar, and P. Alkhairi, "Deep Learning to Extract Animal Images With the U-Net Model on the Use of Pet Images," *J. MEDIA Inform. BUDIDARMA*, vol. 8, no. 1, pp. 468–476, 2024, doi: 10.30865/mib.v8i1.7199.

[24] M. A. Lubis, D. G. S. Saragih, I. D. Anastasia, A. P. Windarto, and P. Alkhairi, "Application of the ANN Algorithm to Predict Access to Drinkable Water in North Sumatra Regency/City," *Int. J. Informatics Data Sci.*, vol. 1, no. 1, pp. 18–25, 2023.

[25] R. Rahad, "A Novel Plasmonic MIM Sensor Using Integrated 1 × 2 Demultiplexer for Individual Lab-on-Chip Detection of Human Blood Group and Diabetes Level in the Visible to Near-Infrared Region," *IEEE Sens. J.*, vol. 24, no. 8, pp. 12034–12041, 2024, doi: 10.1109/JSEN.2024.3372692.

[26] A. Saha, "A Survey of Machine Learning and Meta-heuristics Approaches for Sensor-based Human Activity Recognition Systems," *J. Ambient Intell. Humaniz. Comput.*, vol. 15, no. 1, pp. 29–56, 2024, doi: 10.1007/s12652-022-03870-5.

[27] A. Ferrari, "Deep learning and model personalization in sensor-based human activity recognition," *J. Reliab. Intell. Environ.*, vol. 9, no. 1, pp. 27–39, 2023, doi: 10.1007/s40860-021-00167-w.

[28] T. Zhu, "Multifunctional hydrophobic fabric-based strain sensor for human motion detection and personal thermal management," *J. Mater. Sci. Technol.*, vol. 138, no. 3, pp. 108–116, 2023, doi: 10.1016/j.jmst.2022.08.010.

[29] H. Liang, "Wearable and Multifunctional Self-Mixing Microfiber Sensor for Human Health Monitoring," *IEEE Sens. J.*, vol. 23, no. 3, pp. 2122–2127, 2023, doi: 10.1109/JSEN.2022.3225196.

[30] X. Wang, "Wearable Sensors-Based Hand Gesture Recognition for Human-Robot Collaboration in Construction," *IEEE Sens. J.*, vol. 23, no. 1, pp. 495–505, 2023, doi: 10.1109/JSEN.2022.3222801.

[31] M. A. Khatun, "Deep CNN-LSTM With Self-Attention Model for Human Activity Recognition Using Wearable Sensor," *IEEE J. Transl. Eng. Heal. Med.*, vol. 10, no. 5, pp. 2700316, 2022, doi: 10.1109/JTEHM.2022.3177710.

[32] B. B. Yousif, M. M. Ata, N. Fawzy, and M. Obaya, "Toward an Optimized Neutrosophic k-Means with Genetic Algorithm for Automatic Vehicle License Plate Recognition (ONKM-AVLPR)," *IEEE Access*, vol. 8, no. 3, pp. 49285–49312, 2020, doi: 10.1109/ACCESS.2020.2979185.

[33] M. Yaqub, J. Feng, M. S. Zia, K. Arshid, and K. Jia, "State-of-the-Art CNN Optimizer for Brain Tumor Segmentation in Magnetic Resonance Images," *Brain Sci.*, vol. 10, no. 427, pp. 1–20, 2020, doi: 10.3390/brainsci10070427.

[34] A. Kumar, "Bitcoin Price Prediction Using Sentiment Analysis and Long Short-Term Memory (LSTM)," *Int. J. Intell. Syst. Appl. Eng.*, vol. 11, no. 7, pp. 480–485, 2023.

[35] V. Yadav, "Long short term memory (LSTM) model for sentiment analysis in social data for e-commerce products reviews in Hindi languages," *Int. J. Inf. Technol.*, vol. 15, no. 2, pp. 759–772, 2023, doi: 10.1007/s41870-022-01010-y.

[36] M. Ma, "Predicting machine's performance record using the stacked long short-term memory (LSTM) neural networks," *J. Appl. Clin. Med. Phys.*, vol. 23, no. 3, pp. 1–10, 2022, doi: 10.1002/acm2.13558.

[37] J. Liu, "Prediction of nucleosome dynamic interval based on long-short-term memory network (LSTM)," *J. Bioinform. Comput. Biol.*, vol. 20, no. 3, pp. 11–23, 2022, doi: 10.1142/S0219720022500093.

 ISSN 2723-6471

[38] R. Huang, "Well performance prediction based on Long Short-Term Memory (LSTM) neural network," *J. Pet. Sci. Eng.*, vol. 208, no. 3, pp. 25, 2022, doi: 10.1016/j.petrol.2021.109686.

[39] Y. Kurniawati, "Optimization of Backpropagation Using Harmony Search for Gold Price Forecasting," *Pakistan J. Stat. Oper. Res.*, vol. 18, no. 3, pp. 589–599, 2022, doi: 10.18187/pjsor.v18i3.3915.

[40] T. Yuan, W. Liu, J. Han, and F. Lombardi, "High Performance CNN Accelerators Based on Hardware and Algorithm Co-Optimization," *IEEE Trans. Circuits Syst. I Regul. Pap.*, vol. 68, no. 1, pp. 250–263, 2021, doi: 10.1109/TCSI.2020.3030663.

[41] A. P. Windarto, T. Herawan, and P. Alkhairi, "Prediction of Kidney Disease Progression Using K-Means Algorithm Approach on Histopathology Data," *in Artificial Intelligence, Data Science and Applications, Cham: Springer Nature Switzerland*, vol. 2024, no. 3, pp. 492–497, 2024, doi: 10.1007/978-3-031-48465-0_66.

[42] P. Alkhairi, W. Wanayumini, and B. H. Hayadi, "Analysis of the adaptive learning rate and momentum effects on prediction problems in increasing the training time of the backpropagation algorithm," *AIP Conf. Proc.*, vol. 3048, no. 1, p. 20049, 2024, doi: 10.1063/5.0203374.

[43] K. S. Chong, "Comparison of Naive Bayes and SVM Classification in Grid-Search Hyperparameter Tuned and Non-Hyperparameter Tuned Healthcare Stock Market Sentiment Analysis," *Int. J. Adv. Comput. Sci. Appl.*, vol. 13, no. 12, pp. 90–94, 2022, doi: 10.14569/IJACSA.2022.0131213.

[44] Z. Ragala, A. Retbi, and S. Bennani, "Overview of Gradient Descent Algorithms: Application to Railway Regularity," *in Proceedings of the 8th International Conference on Advanced Intelligent Systems and Informatics 2022, Cham: Springer International Publishing*, vol. 2022, no. 11, pp. 39–49, 2022, doi: 10.1007/978-3-031-20601-6_4.

[45] D. L. M, "An Improved Convolution Neural Network and Modified Regularized K-Means-Based Automatic Lung Nodule Detection and Classification," *J. Digit. Imaging*, vol. 36, no. 4, pp. 1431–1446, 2023, doi: 10.1007/s10278-023-00809-w.

[46] S. Dodia, "A novel receptive field-regularized V-net and nodule classification network for lung nodule detection," *Int. J. Imaging Syst. Technol.*, vol. 32, no. 1, pp. 88–101, 2022, doi: 10.1002/ima.22636.